JOURNAL OF COMPUTATIONAL PHYSICS 56, 469–494 (1984)

A Fourier Method for Three-Dimensional Partial Differential Equations in Periodic Geometry. Application: HELIAC*

A. I. SHESTAKOV AND A. A. MIRIN

National Magnetic Fusion Energy Computer Center, Lawrence Livermore National Laboratory, Livermore, California 94550

Received August 2, 1983; revised January 11, 1984

A numerical method based on Fourier expansions and finite differences is presented. The method is demonstrated by solving a scalar, three-dimensional elliptic equation arising in MFE research, but has applicability to a wider class of problems. The scheme solves equations whose solutions are expected to be periodic in one or more of the independent variables.

1. INTRODUCTION

Numerical solutions to elliptic problems have usually been obtained with finite difference methods. Finite elements have also enjoyed great success in geometries significantly differing from rectangles or boxes. Methods based on expansion of the unknown function in Fourier series are more complicated. Despite the fact that for periodic functions these methods are more "natural," unfortunately, they have not been used as widely.

In this paper we present a hybrid method for three-dimensional problems based on Fourier expansion and finite differences. Although the method has wide applicability, it is illustrated on a specific problem arising in magnetic fusion energy (MFE) research.

The elliptic equation of interest is solved in a coordinate system conforming to the boundary of the domain which is an asymmetric torus. The solution is periodic in two of the angular variables. The entire equation is Fourier-analyzed. Derivatives with respect to the angular variables are expressed exactly using a matrix-vector formulation. Differentiation in the third direction is approximated by finite differences. After the discretization, the harmonics of the solution are algebraically isolated from the harmonics of the coefficients of the equation. The result is a large linear system of equations which is solved by standard methods. The advantage of the

* Work performed under the auspices of the USDOE by the Lawrence Livermore National Laboratory under Contract W-7405-ENG-48.

0021-9991/84 $3.00

581/56/3-8

method is in the economical description of the solution in terms of its Fourier harmonics.

The following section discusses some concepts from MFE research which motivated this work and introduces the application in physical terms. In Section 3, the problem is formulated as a Neumann problem for the scalar potential of a magnetic field. The method and the numerical formulation are presented in Section 4. After introducing a particular coordinate system, the domain becomes similar to that of a periodic cylinder. The coefficients of the equation are Fourier-analyzed and a linear system is derived for the harmonics of the potential. A computer program was written to solve the problem introduced in Section 2. In Section 5, the results of two applications of the method are presented. The cases were chosen to display the wide range of problems which the computer program can handle. Extensions, limitations, a brief discussion and concluding remarks are given in Section 6. Appendix A contains a description of the algorithm used to generate the matrix of harmonics introduced in Section 4. Appendix B gives a mathematical proof justifying the modification of the matrix in Section 4 which guarantees a unique solution.

2. Motivation

Confinement vessels in MFE research usually possess some symmetry. Toroidal devices such as tokamaks and reversed field pinches are toroidally symmetric; theta pinches have azimuthal symmetry. However, present day mirror experiments and stellarators lack this trivial type of symmetry. Interest in stellarators has been revived due to the successes of Wendelstein VII-A at Garching [1]. Although a stellarator is toroidal, the plasma column deviates from toroidal symmetry due to the fields generated by the helically wound coils on the surface of the confinement vessel. The resulting configuration has nested toroidal magnetic surfaces concentric about a magnetic axis that possibly has helical perturbations as it traverses the device. The entire column exhibits the same behavior; it twists as it travels around the torus.

A preliminary step in a proposed experiment is the coil design. Currents in these coils generate the vacuum magnetic field whose usefulness to plasma confinement is then studied. In tokamaks, the coils are of simple structure; hence, the resulting field is easily calculated. Stellarators, having more complicated coil designs, have fields which are harder to compute. Presently, there is great interest in devices in which the helical effects are at least as important as the toroidal ones.

The HELIAC is a proposed device with nested surfaces and a magnetic axis that spirals helically about a circular axis [2]. Such configurations can be constructed by means of various currents running along the major axis, along a circular loop, along a helically wound coil about the circular loop and superimposing a uniform vertical field [3]. Simulations have been performed [2] for a model HELIAC with closed circular coils which are anchored to a larger circular conductor supplying the poloidal field. The center line of the smaller coils traces out a path that helically

winds around the larger circular conductor (Fig. 1). Many variations of the above have been proposed, e.g., whether to have the larger coil link the smaller ones, how many helical periods, etc. One objection to the above configuration is its complexity. It is preferable to have modular coils and to discard the large conductor. The numerical method presented here is applied to the problem of finding simpler coil configurations for HELIAC.

Once the vacuum field is known, its properties are studied. One advantage of HELIAC vs. tokamak vacuum fields is that they may possess an "average magnetic well." This is an extension of the principle behind confinement with magnetic mirrors. Since particles will generally circulate on the magnetic surfaces, configurations are constructed in which the average field increases outward from the magnetic axis, thereby improving confinement. Other aspects studied are the transform and shear of each magnetic surface. The transform, a surface quantity, measures the ratio of the number of poloidal turns per toroidal transit that each field line makes. Shear is a measure of the variation of the transform from one surface to another. Knowledge of the transform is useful in order to avoid surfaces of low order rationality. Such surfaces, where the transform is nearly a ratio of two small integers, will damage the nested topological structure and give rise to large "island" structures [4]. Both the transform and the well depth are computed by following field lines as they travel around the torus. This requires integrating a 3×3 system of ordinary differential equations. At each integration step, the field is evaluated. Consequently, the study of many configurations requires use of an efficient, accurate algorithm for the computation of the field.

There are several approaches to finding optimum HELIAC configurations. If only circular coils are used, the field can be expressed using elliptic integrals. This procedure has been optimized by Ehrhardt [5]. For coils of arbitrary shape, the traditional approach is to fix the coil positions, shapes and currents through the coils.

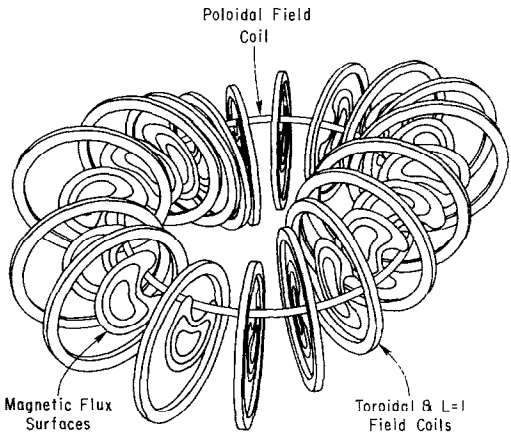

FIG. 1. Proposed coil design for HELIAC. (Courtesy of T. K. Chu, PPPL.)

then use the Biot–Savart law [6] to compute the field. Mai *et al.* [7] use this technique and show that HELIAC can be constructed using only closed poloidal "PACMAN" coils. An alternate approach [8] is to expand the field using a complete set of harmonic functions. If the resulting field properties are deemed favorable, the magnetic field can be regenerated by a set of currents that coincide with the equipotential lines (see [8] and below).

One can consider a few objections to the above methods. The complexity of using only circular coils linked to a larger circular conductor has already been discussed. Disregarding the difficulty of constructing coils of non-standard shapes (e.g., "PACMAN"), the main objection to the Biot–Savart law approach is that the integrations are very slow. The use of the Dommaschk potentials [8] has been successfully applied to the design of Wendelstein VII AS. However, this converges slowly for small aspect ratios. In addition, for HELIAC one must place a singularity of the field at a predetermined position to reproduce the kidney-shaped magnetic surfaces [9]. This singularity is the analogue of the central conductor.

In the alternate approach presented here, we assume the existence of an outer asymmetrical toroidal magnetic surface. The magnetic field inside the surface with non-zero toroidal flux is then computed by the Fourier method described below. As in [8], the field is generated by skin currents flowing on the outer surface. With these means, a large parameter space can be quickly scanned to find optimum HELIAC configurations.

3. Mathematical Formulation

If D is a toroidal domain with boundary ∂D, the problem is to compute the vacuum field $\bar{B}$ in D. This field satisfies:

$$\bar{B} \cdot \hat{n} = 0 \text{ at } \partial D \tag{1}$$

where $\hat{n}$ is the unit outward normal, and

$$\int \bar{B} \cdot \overline{ds} \neq 0 \tag{2}$$

where the integral is over a poloidal cross-section. Since $\bar{B}$ is a vacuum field, it satisfies

$$\nabla \cdot \bar{B} = 0, \qquad \nabla \times \bar{B} = 0 \text{ in } D \tag{3a, b}$$

Using results of Betancourt [10] and Dommaschk [8] we will show that

(a) $\bar{B} = \nabla \psi$ in D, where ψ is the scalar potential.

(b) $\bar{B}$ is generated by surface currents on ∂D.

(c) Once $\bar{B}$ is prescribed outside D, the direction of the surface currents are obtained from the equipotential lines of ψ on ∂D.

(d) These equipotential contours encircle the torus either poloidally or toroidally.

Equation (3b) justifies the ansatz for $\bar{B}$ in (a) above. Equations (3a) and (1) imply that ψ solves a Neumann problem in D. The field, $\bar{B}$, is generated by a current distribution, which is approximated by surface currents on ∂D. Once a configuration is deemed favorable, the surface currents may be discretized into a finite number of closed coils. One is free to specify any additional field, $\bar{B}_{\text{ext}}$, outside the torus; $\bar{B}_{\text{ext}}$ may be given a priori. In the present application, since the search is for a modular coil configuration that lies on ∂D, $\bar{B}_{\text{ext}}$ is set to zero.

Let Δ be a disc with boundary C piercing ∂D and let a, b be two points which mark the intersection of C with ∂D (see Fig. 2).

$$C = C_{ab} + C_{ba}, \qquad \text{where } C_{ab} \text{ lies inside } D \text{ and } C_{ba} \text{ outside.}$$

L_{ab} is the intersection of Δ with ∂D. The total current in ∂D normal to L_{ab} is

$$I_{ab} = \int_{\Delta} (\nabla \times \bar{B}) \cdot \vec{ds} = \oint_{C} \bar{B} \cdot dl = \oint_{C_{ab}} \nabla\psi \cdot dl = \psi(b) - \psi(a), \tag{4}$$

where we assumed that $\bar{B}$ vanished outside. If $a = a_0$ is fixed and b allowed to vary,

$$\psi(b) = I_{ab} + \psi(a_0) = \text{const.} \tag{5}$$

Thus, equipotential lines of ψ on ∂D coincide with surface currents. Another way of proving this is to express the skin current ($=\nabla \times \bar{B}$) in terms of the jump in $\bar{B}$ across the surface; recall that $\bar{B} = \nabla\psi$, and then note that the resulting vector lies on the equipotential lines on the surface. This proves statement (c) following Eqs. (3).

The above analysis is unchanged if $\bar{B}_{\text{ext}} \neq 0$. In this case, the fields inside and outside are respectively expressed as $\bar{B}_{\text{ext}} + \nabla\psi$ and $\bar{B}_{\text{ext}}$. The boundary condition becomes $\partial\psi/\partial n = -\bar{B}_{\text{ext}} \cdot \hat{n}$. The direction of the skin current changes, but it is still coincident with the equipotential lines of ψ. Note that ∂D acts as an insulator to the

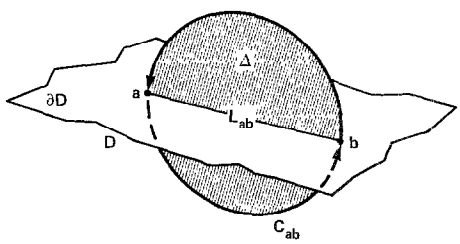

FIG. 2. Section of boundary ∂D showing the disc Δ which pierces ∂D.

total field. Although the solution to the Neumann problem depends on the choice made for $\bar{B}_{ext}$, the resulting field inside D remains unchanged.

The proof that simply connected equipotential lines on ∂D cannot exist is by contradiction. Let C be such a contour. Consider a small volume $V \subseteq D$ (see Fig. 3) bounded by $S = S_c \cup S_\delta \cup S_D$, where S_c is the subsurface of ∂D enclosed by C, S_δ is normal to ∂D and is of small width, and S_D lies inside D on a magnetic surface (an interior surface where $\bar{B} \cdot \hat{n} = 0$). Maxwell's equations imply

$$0 = \int_V \nabla \cdot \bar{B}\, dV = \int_S \bar{B} \cdot \overline{ds} = \int_{S_\delta} \bar{B} \cdot \overline{ds}.$$

The last equality is due to $\bar{B}$ lying parallel to both S_c and S_D. A contradiction arises by recalling that $\bar{B} = \nabla\psi$ and ψ is constant on C; $\bar{B}$ is thus everywhere normal to S_δ, which implies a net flux into V. Due to this contradiction, contours of ψ must encircle the torus either poloidally or toroidally.

The flux condition, Eq. (2), implies that ψ is multiple valued in ϕ, the toroidal angle. If the jump in ψ is set to unity,

$$\psi(\bar{x}(\phi + 2\pi)) - \psi(\bar{x}(\phi)) = 1, \tag{6}$$

the toroidal flux is equal to the magnetic energy. Indeed, consider the simply connected domain D^* of Fig. 4, with boundary Ω_1, Ω_0, and ∂D^*. D^* is a slight alteration of D. An application of Green's first identity to the function ψ gives

$$0 = \int_{D^*} |\nabla\psi|^2\, dV - \int_\Omega [\psi(\bar{x}(\phi + 2\pi)) - \psi(\bar{x}(\phi))] \frac{1}{R} \frac{\partial\psi}{\partial\phi}\, dR\, dZ, \tag{7}$$

where Ω replaces the two domains Ω_1, Ω_0 both lying in constant ϕ planes. The multiple valued nature of ψ is used in deriving (7). Let D^* approach D and invoke Eq. (6); then Eq. (7) implies

$$\text{magnetic energy} = \int_D B^2\, dV = \int_D |\nabla\psi|^2\, dV = 1 \cdot \int_\Omega \bar{B} \cdot \overline{ds} = \text{toroidal flux}. \tag{8}$$

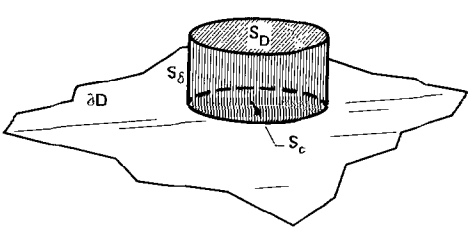

FIG. 3. Section of boundary ∂D as seen from inside D. S_c is a closed simply connected equipotential contour of ψ on ∂D. S_D is a section of a neighboring magnetic surface. Dist $(S_D, S_c) = \delta$ is assumed to be small.

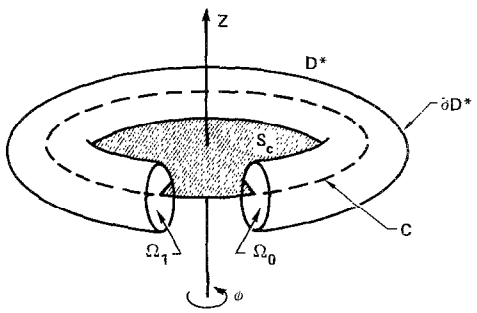

FIG. 4. The simply connected domain D^*. The curve C remains inside D. The boundary of D^* consists of ∂D and the two flat surfaces at $\phi = 0$.

Equation (6) also implies that $\bar{B}$ is generated by a poloidal current on ∂D. In Fig. 4, let C be a contour which encircles the major axis, lies inside D, and encloses a surface S_c. Using Eq. (6), the poloidal current.

$$I_p = \int_{S_c} \overline{ds} \cdot (\nabla \times \bar{B}) = \int_C \bar{B} \cdot \overline{dl} = \int_C \nabla\psi \cdot \overline{dl}$$
$$= \psi(\bar{x}(\phi + 2\pi)) - \psi(\bar{x}(\phi)) = 1. \tag{9}$$

The lack of periodicity of ψ is easily removed and leads to the formulation of the Neumann problem:

Let

$$\psi \equiv \chi + \phi/2\pi \tag{10}$$

where

$$\nabla^2\chi = 0 \qquad \text{in } D \tag{11a}$$

$$\frac{\partial\chi}{\partial n} = -\frac{1}{2\pi R}\hat{\phi} \cdot \hat{n} \qquad \text{on } \partial D. \tag{11b}$$

The potential χ is periodic in ϕ. Equations (10) and (11b) assure the satisfaction of Eq. (1). The Neumann problem for χ, Eqs. (11), is mathematically well posed. The boundary function in Eq. (11b) satisfies the compatibility condition [11], for using an application of Green's identity,

$$\int_{\partial D} \frac{1}{R}\hat{\phi} \cdot \hat{n}\, dA = \int_{\partial D} \frac{\partial\phi}{\partial n} dA = \int_D \nabla^2\phi\, dV = 0.$$

The last equality follows since ϕ is a harmonic function. The potential χ is unique up to an additive constant.

4. Numerical Implementation

In this section we discuss the numerical method which solves the Neumann problem for χ introduced in the last section.

We begin by describing the coordinate system. These coordinates are not orthogonal and not standard. However, with some modifications they are applicable to any toroidal geometry. Two of the variables are angular. Their introduction allows the expansion of any single valued function in a double Fourier series. The third is a scaled radial distance. Its definition implies that the boundary, ∂D, is a coordinate plane, thus, ensuring a good approximation of the boundary condition given by Eq. (11b).

In the second subsection the Fourier expansion method is introduced. A discussion of the algebra and calculus of the discretization follows. The section ends by a description of the linear system for the harmonics of the solution. Since the solution is unique only up to an additive constant the matrix is singular. One of its equations is modified to ensure solvability. A mathematical justification of this is given in Appendix B.

A. *Derivation of Equations in the Appropriate Coordinate System*

The domain of interest, D, consists of the interior of a torus swept out by a two-dimensional cross-section that is helically wound about a circular axis. Specifically, consider the contour $f(R, Z) = 0$ of Fig. 5. D is then the volume enclosed by the contour as it is rigidly wound about the circle of radius R_0 according to the winding law, $\theta(\phi)$. We now define R_0 as the major radius, ρ as the winding radius, $\theta(\phi)$ as the winding law (e.g., $\theta(\phi) = k\phi$, k integer), ϕ as the toroidal angle, ζ as the poloidal angle and τ as the radial variable. In the (τ, ϕ, ζ) coordinate system (not orthogonal), ∂D is given by $\tau = g(\zeta)$ where g is periodic in ζ.

Define the scaled radial displacement

$$\sigma = \tau / g(\zeta); \tag{12}$$

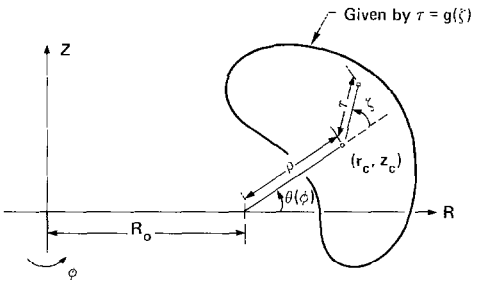

FIG. 5. Definition of τ, ϕ, ζ coordinates.

then $0 \leqslant \sigma \leqslant 1$ and $\sigma = 1$ defines the boundary. The coordinate transformation is

$$\begin{aligned} R &= R_0 + \rho \cos \theta(\varphi) + \sigma g(\zeta) \cos(\theta(\phi) + \zeta), \\ \phi &= \phi, \\ Z &= \rho \sin \theta(\phi) + \sigma g(\zeta) \sin(\theta(\phi) + \zeta), \end{aligned} \tag{13}$$

with Jacobian $J = (\sigma g(\zeta)^2 R)^{-1}$.

The coordinates of interest are (σ, ϕ, ζ). Since HELIAC is allowed m_h helical periods per toroidal transit, the domain is

$$D = \{(\sigma, \phi, \zeta): 0 \leqslant \sigma \leqslant 1; 0 \leqslant \zeta < 2\pi; 0 \leqslant \phi < 2\pi/m_h\}. \tag{14}$$

In (σ, ϕ, ζ) coordinates, the equation to solve is

$$\begin{aligned} 0 = \nabla^2 \chi = \sigma g(\zeta)^2 R \cdot \Big\{ & \frac{\partial}{\partial \sigma}\left(a \frac{\partial \chi}{\partial \sigma} + b \frac{\partial \chi}{\partial \phi} + c \frac{\partial \chi}{\partial \zeta}\right) \\ & + \frac{\partial}{\partial \phi}\left(b \frac{\partial \chi}{\partial \sigma} + d \frac{\partial \chi}{\partial \phi} + e \frac{\partial \chi}{\partial \zeta}\right) + \frac{\partial}{\partial \zeta}\left(c \frac{\partial \chi}{\partial \sigma} + e \frac{\partial \chi}{\partial \varphi} + f \frac{\partial \chi}{\partial \zeta}\right) \Big\}, \end{aligned} \tag{15}$$

where

$$\begin{aligned} a &= \sigma \left\{ 1 + \left[\frac{g'(\zeta)}{g(\zeta)}\right]^2 \right\} R + \sigma \left(\frac{V(\sigma, \zeta)\, \theta'(\phi)}{g(\zeta)}\right)^2 \left(\frac{1}{R}\right), \\ b &= \sigma V(\sigma, \zeta)\, \theta'(\phi)/R, \\ c &= -R g'(\zeta)/g(\zeta) - (\sigma + \rho \cos \zeta / g(\zeta)) \left(\frac{V(\sigma, \zeta)\, \theta'(\phi)^2}{R}\right), \\ d &= \sigma g(\zeta)^2 / R, \\ e &= -g(\zeta)[\sigma g(\zeta) + \rho \cos \zeta]\, \theta'(\phi)/R, \\ f &= R/\sigma + \theta'(\phi)^2 (\sigma g(\zeta) + \rho \cos \zeta)^2 / (R\sigma), \\ V(\sigma, \zeta) &= \frac{\partial}{\partial \zeta} [\sigma g(\zeta)^2/2 + \rho g(\zeta) \cos \zeta], \end{aligned} \tag{16}$$

and R is given by Eq. (13).

Equation (11b) may be derived in the (σ, ϕ, ζ) coordinates by computing $\nabla \psi \cdot \nabla \sigma = 0$ or equivalently by deriving $\nabla \psi \cdot \nabla Y = 0$ where $Y \doteq \tau - g(\zeta)$ is a function constant on ∂D. The boundary condition becomes

$$a_1 \frac{\partial \chi}{\partial \sigma} + b_1 \frac{\partial \chi}{\partial \phi} + c_1 \frac{\partial \chi}{\partial \zeta} = -\frac{b_1}{2\pi}. \tag{17}$$

where

$$
\begin{aligned}
a_1 &= 1 + [g'(\zeta)/g(\zeta)]^2 + [W(\zeta)\,\theta'(\phi)/R]^2, \\
b_1 &= -g(\zeta)\,W(\zeta)\,\theta'(\phi)/R^2, \\
c_1 &= -g'(\zeta)/g(\zeta) + W(\zeta)[g(\zeta) + \rho\cos\zeta]\left[\frac{\theta'(\phi)}{R}\right]^2, \\
W(\zeta) &= -\left\{\frac{d}{d\zeta}\left[\frac{1}{2}\,g(\zeta)^2 + \rho g(\zeta)\cos\zeta\right]\right\}\Big/ g(\zeta).
\end{aligned}
\tag{18}
$$

In Eqs. (15)–(18) both χ, the unknown, and $a, b, \ldots, a_1, b_1, c_1$, the coefficients, are periodic in ϕ with period $2\pi/m_h$ and periodic in ζ with period 2π. The coefficients depend on input quantities such as $g(\zeta)$ and $\theta(\phi)$.

Equation (15) is homogeneous, while the r.h.s. of (17) depends on $\theta'(\phi)$. It is worth noting that an axisymmetric torus of arbitrary cross-section has $\theta'(\phi) = 0$, giving a homogeneous boundary condition. This implies that the only solution is given by $\psi = \phi/2\pi + \text{const.}$, i.e., $\bar{B} \sim \nabla\phi = (1/R)\hat{\phi}$, a purely toroidal field equivalent to the one induced by a uniform current along the Z-axis.

The solution χ is unique up to an additive constant. Since χ is single valued and periodic in both ζ and ϕ, at $\sigma = 0$ it is independent of ζ; i.e.,

$$
\chi(\sigma = 0) = \chi_{\text{av}} + \sum_k \chi_{0,k} \exp(ikm_h\phi). \tag{19}
$$

The potential χ is made unique by specifying its mean value at $\sigma = 0$,

$$
\chi_{\text{av}} = 0. \tag{20}
$$

At $\sigma = 0$, the Jacobian of the coordinate system is singular; the poloidal variable ζ loses its meaning. However, the Laplacian operator is still valid and the solution is regular there. We derive another relationship for χ by integrating the partial differential equation over a small disc centered at $\sigma = 0$. Recalling Eq. (15),

$$
\begin{aligned}
0 &= L(\chi) = \mathrm{I} + \mathrm{II} + \mathrm{III} \text{ where} \\
\mathrm{I} &\equiv \frac{\partial}{\partial\sigma}\left(a\frac{\partial\chi}{\partial\sigma} + b\frac{\partial\chi}{\partial\phi} + c\frac{\partial\chi}{\partial\zeta}\right), \\
\mathrm{II} &\equiv \frac{\partial}{\partial\phi}\left(b\frac{\partial\chi}{\partial\sigma} + d\frac{\partial\chi}{\partial\phi} + e\frac{\partial\chi}{\partial\zeta}\right), \\
\mathrm{III} &\equiv \frac{\partial}{\partial\zeta}\left(c\frac{\partial\chi}{\partial\sigma} + e\frac{\partial\chi}{\partial\phi} + f\frac{\partial\chi}{\partial\zeta}\right).
\end{aligned}
\tag{21}
$$

Choose $\delta > 0$ and integrate

$$0 = \int_0^{\delta} d\sigma \int_0^{2\pi} d\zeta\, L(\chi) = \iint (\mathrm{I} + \mathrm{II} + \mathrm{III}). \tag{22}$$

The third integral in Eq. (22) vanishes by periodicity, i.e.,

$$\iint \mathrm{III} = \int d\sigma \int_0^{2\pi} d\zeta \frac{\partial}{\partial \zeta}(\ ) = 0. \tag{23}$$

For $\int \mathrm{I}$, the order of integration is interchanged and

$$\int \mathrm{I} = \int_0^{2\pi} d\zeta \left(a \frac{\partial \chi}{\partial \sigma} + b \frac{\partial \chi}{\partial \phi} + c \frac{\partial \chi}{\partial \zeta} \right) \Bigg|_{\sigma=0}^{\delta}. \tag{24}$$

However, $\partial\chi/\partial\sigma$ and $\partial\chi/\partial\phi$ are bounded at $\sigma = 0$ and $a, b \sim \sigma$. A simple analysis shows $\partial\chi/\partial\zeta \sim \sigma$. Thus, the integrand in Eq. (24) needs to be evaluated only at $\sigma = \delta$. The third term in Eq. (24) is then integrated by parts which gives

$$\int \mathrm{I} = \int_0^{2\pi} d\zeta \left(a \frac{\partial \chi}{\partial \sigma} + b \frac{\partial \chi}{\partial \phi} - \frac{\partial c}{\partial \zeta} \chi \right) \Bigg|_{\sigma=\delta}. \tag{25}$$

The second term in Eq. (22) is a sum of three parts, $\mathrm{II} = \mathrm{II} \cdot 1 + \mathrm{II} \cdot 2 + \mathrm{II} \cdot 3$; e.g., $\mathrm{II} \cdot 3 = \partial(e\, \partial\chi/\partial\zeta)/\partial\phi$. These three terms are analysed as above.

The result gives the integral equation for χ:

$$\int_0^{2\pi} d\zeta \left[a \frac{\partial \chi}{\partial \sigma} + b \frac{\partial \chi}{\partial \phi} - \frac{\partial c}{\partial \zeta} \chi + \left(\frac{\Delta\sigma}{4} \right) \frac{\partial}{\partial \phi} \left(b \frac{\partial \chi}{\partial \sigma} + d \frac{\partial \chi}{\partial \phi} - \frac{\partial e}{\partial \zeta} \chi \right) \right] \Bigg|_{\sigma = \Delta\sigma/2} = 0. \tag{26}$$

B. *Fourier Expansion Method*

Since both the coefficients of the equation and the solution are periodic with respect to ϕ and ζ, they possess Fourier expansions, e.g.,

$$\begin{aligned} f(\sigma, \phi, \zeta) &= \sum_{k,l} f_{k,l}(\sigma) \exp(i(k\phi + l\zeta)) \\ &= f_{0,0} + f_{0,1} \cos\zeta + f_{0,2} \sin\zeta + \cdots + f_{0,M} \sin m\zeta \\ &\quad + (f_{1,0} + f_{1,1} \cos\zeta + f_{1,2} \sin\zeta + \cdots + f_{1,M} \sin m\zeta) \cos\phi \\ &\quad + (f_{2,0} + f_{2,1} \cos\zeta + \cdots + f_{2,M} \sin m\zeta) \sin\phi \\ &\quad + \cdots + (f_{N,0} + f_{N,1} \cos\zeta + \cdots + f_{N,M} \sin m\zeta) \sin n\phi. \end{aligned} \tag{27}$$

In this expression, the series is truncated at m, n and we define $M = 2m$, $N = 2n$.

There are $(N+1)(M+1)$ harmonics for each σ. The harmonics $f_{k,l}$ are functions of σ. The HELIAC configuration has m_h helical periods. In this case, ϕ in Eq. (27) is replaced by $m_h\phi$. If f is a known function, Fourier transforming yields the $f_{k,l}$. The method presented here shows how to compute the harmonics $\chi_{k,l}$ for the unknown χ.

For fixed σ, two doubly periodic functions a and χ can be identified with $\bar{a}$ and $\bar{\chi}$, the vectors whose components are the harmonics $a_{k,l}$ and $\chi_{k,l}$, respectively. The product of two such functions can be represented in matrix vector form: $A\,\bar{\chi}$, where A is a square matrix of order $(N+1)(M+1)$. The elements of A consist of the components of $\bar{a}$. If a is known while χ is unknown, the harmonics of χ are algebraically isolated, e.g., if

$$\bar{a} = (a_0, a_1, a_2) = a_0 + a_1 \cos x + a_2 \sin x,$$

$$\bar{\chi} = (\chi_0, \chi_1, \chi_2) = \chi_0 + \chi_1 \cos x + \chi_2 \sin x,$$

$$A\bar{\chi} = \begin{bmatrix} a_0 & \frac{1}{2}a_1 & \frac{1}{2}a_2 \\ a_1 & a_0 & 0 \\ a_2 & 0 & a_0 \end{bmatrix} \begin{bmatrix} \chi_0 \\ \chi_1 \\ \chi_2 \end{bmatrix}.$$

The truncation error is: $\frac{1}{2}(a_1\chi_1 - a_2\chi_2)\cos 2x + \frac{1}{2}(a_1\chi_2 + a_2\chi_1)\sin 2x$. The appendix presents the algorithm that generates A for arbitrary n and m.

The harmonics of $f(\phi, \zeta)$ are stored in vector form,

$$\bar{f} = (f_{0,0}, f_{0,1}, \ldots, f_{0,M}, f_{1,0}, \ldots, f_{N,M}) \tag{27a}$$

where $\dim(\bar{f}) = (N+1)(M+1)$. Differentiation with respect to ϕ or ζ is expressed in matrix vector form with infinite accuracy (for the representation chosen for $\bar{f}$):

$$\frac{\partial \bar{f}}{\partial \phi} = m_h P_\phi \bar{f} \qquad \text{and} \qquad \frac{\partial \bar{f}}{\partial \zeta} = P_\zeta \bar{f}.$$

Here m_h is the number of helical periods per toroidal transit. The matrices P_ϕ, P_ζ are of order $(N+1)(M+1)$. In block form,

$$P_\phi = \begin{bmatrix} 0 & 0 & & & & \\ 0 & 0 & I_m & & & \\ & -I_m & 0 & 0 & & \\ & & 0 & 0 & 2I_m & \\ & & & -2I_m & 0 & 0 \\ & & & & 0 & \cdot \\ & & & & & \cdot \end{bmatrix}. \tag{28}$$

and I_m is the identity matrix of order $M+1$. The matrix $P_\zeta = \mathrm{diag}(p_\zeta)$ where

$$p_\zeta = \begin{bmatrix} 0 & 0 & & & & \\ 0 & 0 & 1 & & & \\ & -1 & 0 & 0 & & \\ & & 0 & 0 & 2 & \\ & & & -2 & \cdot & \\ & & & & & \cdot \end{bmatrix} \tag{29}$$

and order $(p_\zeta) = M+1$.

C. *Discretization of Equations*

The equations to solve are Eq. (15) for $\Delta\sigma \leqslant \sigma \leqslant 1$, Eq. (17) for $\sigma = 1$, and Eq. (26) where χ at $\sigma = 0$ is given by Eqs. (19) and (20). Divide the interval $0 \leqslant \sigma \leqslant 1$ into L subintervals $0 = \sigma_0 < \sigma_1 < \cdots < \sigma_L = 1$. Differentiations with respect to σ are approximated by finite differences. At $\sigma = \sigma_j$, let χ_j denote the vector of harmonics corresponding to the unknown function $\chi(\sigma_j)$, and let $A_j, B_j, \ldots$ respectively denote the matrices resulting by properly combining the harmonics of the vectors $\bar{a}_j, \bar{b}_j, \ldots$ corresponding to the coefficients $a, b, \ldots$ (see Appendix A). Divide Eq. (15) by $\sigma g(\zeta)^2 R$ and discretize at $\sigma = \sigma_j$, $j = 1, 2, \ldots, L$:

$$\begin{aligned} &\left(\frac{2}{\sigma_{j+1} - \sigma_{j-1}}\right) A_{j+1/2}(\chi_{j+1} - \chi_j)/(\sigma_{j+1} - \sigma_j) \\ &\quad + (m_h B_{j+1/2} P_\phi + C_{j+1/2} P_\zeta)\chi_{j+1/2} - \cdots \\ &\quad + m_h P_\phi B_j(\chi_{j+1} - \chi_{j-1})/(\sigma_{j+1} - \sigma_{j-1}) + m_h D_j P_\phi \chi_j + \cdots + P_\zeta[\cdots] = 0. \end{aligned} \tag{30}$$

Note that the matrices P_ϕ, P_ζ multiply the coefficient matrices either on the left or right, corresponding to differentiated terms such as $\partial(b\chi)/\partial\phi$ or $b\partial\chi/\partial\phi$, respectively. In Eq. (30), $\chi_{j+1/2} = (\chi_{j+1} + \chi_j)/2$. Equation (30) is rearranged in the form

$$Q_j\chi_{j-1} + S_j\chi_j + T_j\chi_{j+1} = 0, \qquad j = 1, 2, \ldots, L, \tag{31}$$

which is a block tri-diagonal system of equations. In Eq. (31),

$$Q_j \doteq \left(\frac{2}{\Delta\sigma_{j-1/2}}\right) A_{j-1/2} - G_j - C_{j-1/2} P_\zeta, \tag{32a}$$

$$\begin{aligned} S_j \doteq\ & 2\Delta\sigma_j [P_\zeta F_j P_\zeta + m_h(P_\phi E_j P_\zeta + E_j P_\zeta P_\phi) + m_h^2 D_j P_\phi P_\phi] \\ & + (C_{j+1/2} - C_{j-1/2}) P_\zeta - 2(A_{j+1/2}/\Delta\sigma_{j+1/2} + A_{j-1/2}/\Delta\sigma_{j-1/2}), \end{aligned} \tag{32b}$$

$$T_j \doteq \left(\frac{2}{\Delta\sigma_{j+1/2}}\right) A_{j+1/2} + G_j + C_{j+1/2} P_\zeta \tag{32c}$$

where P_ϕ, P_ζ are given in Eqs. (28), (29) above,

$$G_j = P_\zeta C_j + m_h(P_\phi B_j + B_j P_\phi) \qquad \text{and}$$
$$\Delta\sigma_{j+1/2} = \sigma_{j+1} - \sigma_j, \qquad \Delta\sigma_j = (\sigma_{j+1} - \sigma_{j-1})/2. \tag{32d}$$

Equation (17) is similarly discretized at $\sigma = \sigma_L = 1$:

$$-A_{1,L}\chi_{L-1} + D_{1,L}\chi_L + A_{1,L}\chi_{L+1} = -(\Delta\sigma_L/\pi)\bar{b}_1 \tag{33}$$

where

$$D_{1,L} = (2\Delta\sigma_L)(m_h B_{1,L} P_\phi + C_{1,L} P_\zeta) \tag{34}$$

and $A_{1,L}, B_{1,L} C_{1,L}$ are the matrices which respectively correspond to the coefficients a_1, b_1 and c_1 in Eq. (17). The vector of harmonics $\bar{b}_1$ in Eq. (33) contains the [illegible] eliminate χ_{L+1}. This gives

$$[A_{1,L} T_L^{-1} Q_L + A_{1,L}]\chi_{L-1} + [A_{1,L} T_L^{-1} S_L - D_{1,L}]\chi_L = (\Delta\sigma_L/\pi)\bar{b}_1. \tag{35}$$

A similar procedure is performed at $\sigma = 0$. Equation (26) is discretized and combined with Eq. (31) (for $j = 1$). The procedure is altered due to the specification of χ_{av} at $\sigma = 0$ (Eqs. (19) and (20)). As discussed above, this specification is made to remove the non-uniqueness of the solution of the Neumann problem. The procedure is simplified if a Dirichlet problem needs to be solved, since χ_{av} then cannot be given a priori. Discretizing Eq. (26) gives

$$0 = \int_0^{2\pi} d\zeta[(A_{0,0} + B_{0,0})\chi_1 + (-A_{0,0} + B_{0,0})\chi_0] \tag{36}$$

where

$$A_{0,0} = (2/\Delta\sigma) A_{1/2} + (m_h/2) P_\phi B_{1/2}, \tag{37a}$$

and

$$B_{0,0} = -[P_\zeta \bar{c}_{1/2}] + m_h \left(B_{1/2} P_\phi - \frac{\Delta\sigma}{4} P_\phi [P_\zeta \bar{e}_{1/2}]\right) + m_h^2 \left(\frac{\Delta\sigma}{4}\right) P_\phi D_{1/2} P_\phi. \tag{37b}$$

In the above equations, $A_{1/2}, B_{1/2}$,... correspond to the matrices generated by the harmonics of the coefficients a, b,... in Eq. (15) evaluated at $\sigma = \Delta\sigma/2$. The two terms enclosed by square brackets in Eq. (37b) denote the matrices corresponding to the enclosed vectors; the vectors $c_{1/2}$, $e_{1/2}$ correspond to the coefficients c and e. Finally χ_1 and χ_0 represent the vector of harmonics of χ at $\sigma = \Delta\sigma$ and 0 respectively.

In Eq. (36), the integral is a vector of harmonics. If the harmonics in χ_j are ordered as in Eq. (27), and stored as in Eq. (27a), then for

$$i = j(M+1) + 1, \qquad j = 0, 1, \ldots, N, \tag{38}$$

the f_i harmonics correspond to terms independent of ζ. At $\sigma = 0$, all other harmonics vanish to assure single-valuedness. If only these f_i harmonics of the integrand are considered, the integration is trivial. Let H_0 denote the square submatrix of order $N+1$ consisting of only the elements of $B_{0,0} - A_{0,0}$ that belong to both rows i and columns i, for i defined in Eq. (38). Let K_0 denote the $(N+1) \times (N+1)(M+1)$ submatrix consisting of only rows i of $A_{0,0} + B_{0,0}$. Equation (36) becomes

$$H_0 x_0 + K_0 \chi_1 = 0 \tag{39}$$

where the sub-vector x_0 has $\dim(x_0) = N+1$ and contains only the i harmonics of χ_0.

If one is interested in solving the Dirichlet problem, Eq. (39) may be combined with Eq. (31) (for $j = 1$) thereby eliminating χ_0, giving

$$(S_1 - \tilde{Q}_1 H_0^{-1} K_0)\chi_1 + T_1 \chi_2 = 0 \tag{40}$$

where $\tilde{Q}_1$ is a rectangular matrix of dimension $(N+1)(M+1) \times (N+1)$ consisting of the i columns of Q_1 for i defined in Eq. (38). However, for the Neumann problem, Eq. (20) must also be considered. Our procedure, to be justified in Appendix B, replaces the first row of Eq. (39) with the discretization of Eq. (20). The entire first row of K_0 is set to zero. In addition, the entire first row of H_0 is also set to zero except for the (1, 1) element which is set to one.

Combining Eqs. (40), (35), and (31) for $j = 2, 3, \ldots, L-1$ gives a block-tridiagonal system of equations for the unknowns χ_j, $j = 1, 2, \ldots, L$. This system may be solved by standard banded or block-tridiagonal solvers. In our applications we use BTMS [12], a version of standard block-tridiagonal gauss reduction which needs approximately 1/3 of the storage that the entire matrix would require. Later applications requiring more harmonics to represent the boundary use DSBTMS [13]. This is a disc version of the above routine with a storage requirement equivalent to one block row of the matrix.

5. Computational Results

In this section, we present two applications that illustrate the generality of the method. Both cases model proposed or existing expeiments. The relevant parameters for the cases presented are given in Table I. A wide parameter study is published elsewhere [14].

Once the harmonics are computed, they are given to a field line tracing code, TUBE [15], which integrates the system of ordinary differential equations,

$$dr/dl = B_r/B, \qquad dz/dl = B_z/B, \qquad d\phi/dl = B_\phi/rB \tag{41}$$

where B_i is the i-th component of $\vec{B}$ $(=\nabla\psi)$ (cylindrical coordinates) and $B = |\vec{B}|$. The independent variable is l, the length along a field line. The three dependent variables (r, ϕ, z) are the cylindrical coordinates of the field line. This integration

TABLE I

Relevant Parameters for Computational Results

Case	1	2
R_0	9	9
ρ	1.2	0
$\theta(\phi)$	$2\phi - (1/4)\sin 2\phi$	2ϕ
$g(\zeta)$	(1, −.073, −.3165, .1193)	(1, 0, 0, .15, 0, 0, .02)

Note. Definitions of variables are given in the text preceding Eq. (12) and in Fig. 5. For $g(\zeta)$, only the $\cos k\zeta$ harmonics $k = 0, 1, \ldots$ are listed. Thus, for Case 1, $g(\zeta) = 1 - .073\cos\zeta - .3165\cos 2\zeta + .1193\cos 3\zeta$.

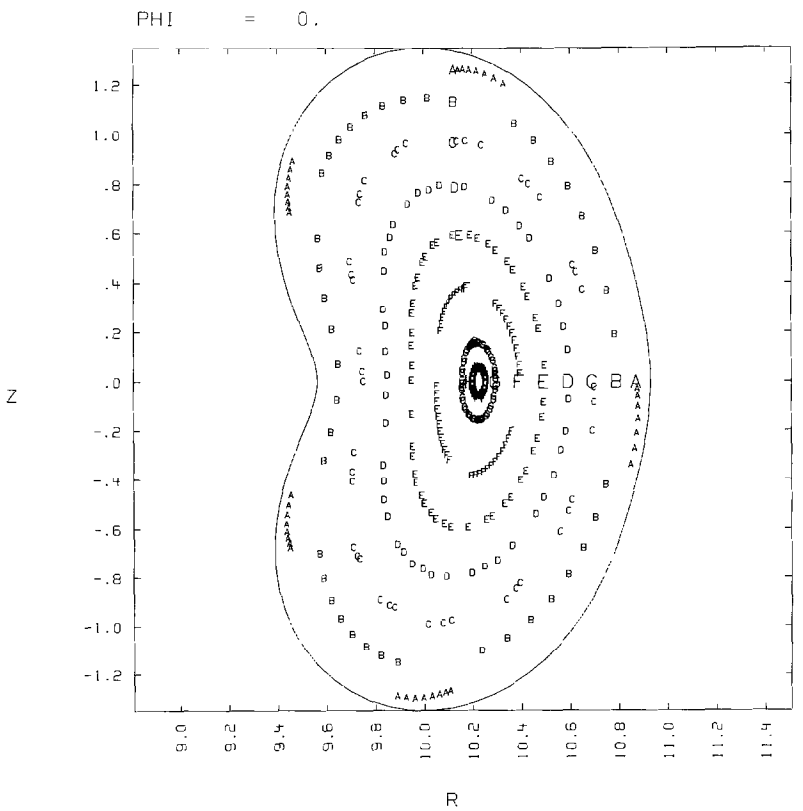

FIG. 6. Field line tracing plot of HELIAC model. Boundary of D is the bean-like contour adjoining the symbols A.

requires computing the three components of $\nabla\psi$. Each intersection of the field line with a symmetry plane is recorded and plotted in Figs. 6 and 7. Magnetic surfaces are traced by joining all positions of the same letter. On each surface the average value of $1/B$ and the transform are also computed.

Case 1, a HELIAC, has the bean-like cross-section outlined in Fig. 6. The aspect ratio is ~9. The helical twist is at least as important as the toroidal curvature. The choice for $\theta(\phi)$ made in Table I imposes two helical periods per toroidal transit. It also has the effect that the cross-section spends more time outside the circle of radius R_0 than inside. This modulation of $\theta(\phi)$ is found to produce configurations with deeper magnetic wells [14]. Figure 8 is a three-dimensional plot of one helical period. The grid lines on the surface correspond to constant ϕ and ζ angles. The rings are equipotential contours and coincide with the direction of the skin currents that generate the field. Note that the currents are tilted in the direction of the pitch of the helix. A closer inspection (not evident from the figure) shows that the current loops

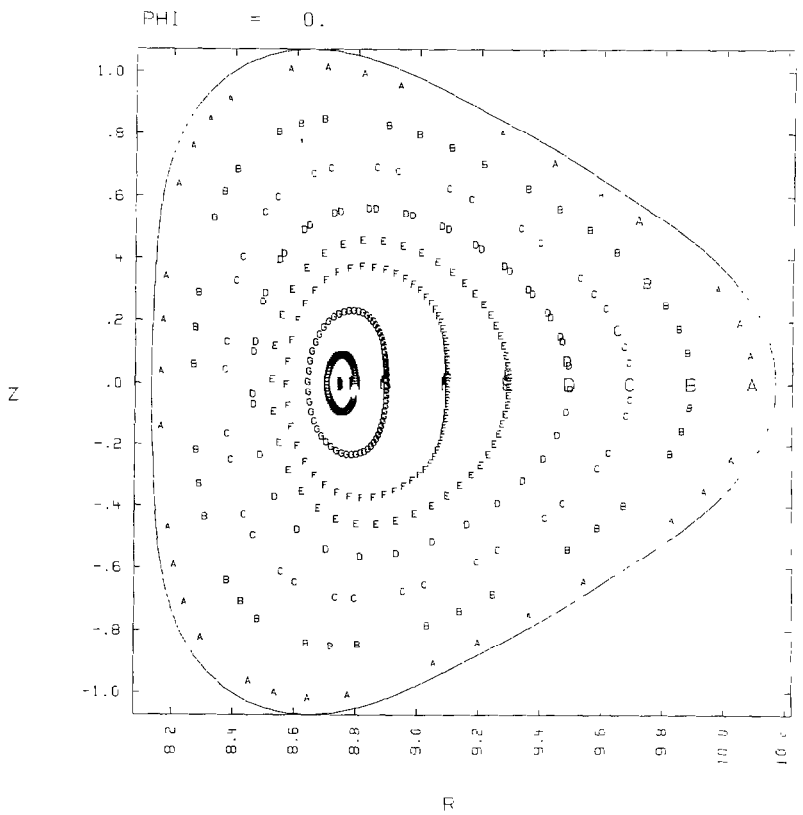

FIG. 7. Field line tracing plot of stellarator model. Boundary of D is the triangular contour adjoining the symbols A.

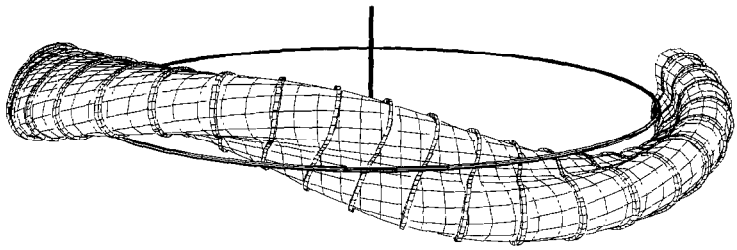

FIG. 8. 3-Dimensional plot of boundary of HELIAC showing one field period. Grid on the surface shows constant ϕ and constant ζ lines. The rings show direction of skin currents. Outlined circular axis and major axis are for reference only. (Courtesy of N. J. O'Neill, MFECC LLNL.)

are not planar. This configuration has a slight magnetic well (~1.3%) and moderate shear. Results are displayed in Fig. 9.

Case 2 demonstrates the applicability of this method to standard stellarators. We use parameters approximating CLEO [16]. In this case ρ, the winding radius, is zero. Although $\theta(\phi) = 2\phi$, the three-fold symmetry of $g(\zeta)$ and choice for ρ (=0) gives six helical periods per toroidal transit. Figure 7 is a field line tracing plot of this configuration. Figure 10 displays the average field strength and the transform. The configuration has a magnetic hill and little shear. Note that the magnetic axis, which at $\phi = 0$, $Z = 0$, is at $R = 8.75$, is distinct from the axis of the (σ, ϕ, ζ) coordinate system which lies at $R = 9$.

The above cases were run on the CRAY-1S computer at the National MFE Computer Center at Livermore. This machine has approximately 1.2 million decimal words available for the user. Approximately 80% of the time is spent in computing the matrix coefficients; the remaining time is used by the Gaussian elimination matrix solver. The run time to compute ψ is approximately $0.0093L(MN)^{1.6}$ seconds where L, M, N respectively denote, the maximum number of σ mesh points, and the highest ζ and ϕ harmonics carried. Typical values are $L = 40$, $M = 12$, $N = 3$. In addition, approximately 60–90 seconds is required for the field line integrator TUBE [15] to examine the field.

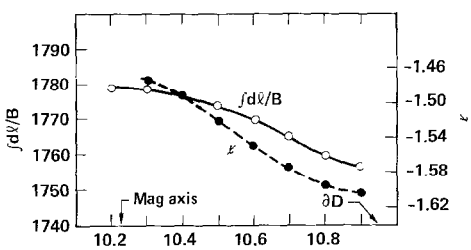

FIG. 9. HELIAC Model. Average inverse field strength, $\int dl/B$, and transform, ι, vs. R, the distance from the major axis at $\phi = 0$, $Z = 0$. Location of the boundary and magnetic axis is shown.

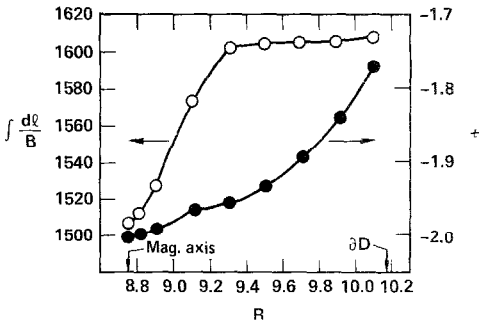

FIG. 10. Stellarator Model. Average inverse field strength, $\int(dl/B)$, and transform ι, vs R, dist. from the major axis at $\phi = 0$, $Z = 0$. Location of the boundary and magnetic axis is shown.

6. EXTENSIONS, LIMITATIONS, DISCUSSION AND CONCLUSIONS

The computer program has been modified for the cases of interest in HELIAC

$$g(\zeta) = \sum_k g_k \cos k\zeta.$$

Furthermore, the winding law is $\theta(\phi) = k\phi$ or possibly $\theta(\phi) = k\phi + \varepsilon \sin k\phi$ (k integer). The resulting ψ has a symmetry which requires computation and storage of only half of the harmonics. Taking advantage of this allows the use of more complicated cross-sections, σ-mesh points, etc.

In the present application, the limitations of the method stem from its demands for large computer memory. If a typical $g(\zeta)$ is to carry $m/2$ harmonics, (cosine and sine included), the solution needs $\sim m$ harmonics (possibly more, if the harmonics of g do not decay rapidly). If $M = 2m$, then $(M + 1)$ harmonics of ζ are required. Similarly, if ψ carries up to n ϕ-terms, and $N = 2n$, $N + 1$ toroidal terms need to be computed. The sub-matrices appearing in Eq. (31) are of order $(N + 1)(M + 1)$. The entire block tridiaginal matrix will contain $\sim 3L(N + 1)^2(M + 1)^2$ elements where L is the number of block rows. The DSBTMS solver [13] is very useful since it reduces the storage requirement by a factor of L. Furthermore, taking advantage of the aforementioned symmetry, the requirement is reduced by another factor of four. The significant storage limitation stems from the algorithm which computes the matrix coefficients. At present 9 blocks of $(N + 1)^2(M + 1)^2$ elements are required.

Computer time is not a significant factor. Hundreds of configurations can be tested using modest amounts of time. This approach is superior to the standard method of coil design using the Biot–Savart law. Running times using the Biot–Savart law increase rapidly with both the number and complexity of the coils. It is not uncommon to spend 5–10 minutes of equivalent CRAY time to compute just one flux surface.

A few words should be said regarding the choice of coordinates. The development of the method grew out of a desire to compute the vacuum field inside an asym-

metrical torus. A cylindrical coordinate system was inappropriate since the domain of definition in those coordinates is nontrivial. We were thus led to a (τ, ϕ, ζ) system whose axis lies inside the domain. Introduction of the scaled distance σ $(=\tau/g(\zeta))$ facilitated an accurate discretization of the boundary condition. After deriving Eq. (15), one could use a finite difference approximation to all of the derivatives. This, however, leads to a very large sparse matrix with few available routines to invert it. On the other hand, the (σ, ϕ, ζ) system has the advantage that the solution is doubly periodic in these coordinates. Thus, one is irresistibly drawn to a Fourier representation of the functions. The double Fourier expansion has the added attraction that the resulting system is of block tridiagonal form with full blocks. For such systems there are readily available routines [12, 13].

Some skeptics point out that a Fourier representation is useful and economical, only when one predetermines an optimal angular variable. We concur to a degree. In the applications presented here, we rarely used more than three toroidal harmonics $(n = 3)$. This gives evidence that ϕ is a good toroidal variable. However, on occasion, as many 20 poloidal harmonics $(m = 20)$ were needed. Apparently, ζ is not a good poloidal variable [17]. One can experiment with other variables, e.g., $u = \zeta + F(\zeta)$ where F is periodic in ζ. It is straightforward, but tedious to incorporate the new definition into the equations. The Fourier method, however, can be applied as before.

Lastly, the numerical method can be used in other physical applications. In particular, it can solve any elliptic problem when the solution and the coefficients have any number of periodic independent variables. Non-linear problems would, of course, require iteration. The coordinate system used is not essential to the applicability of the method. One may consider the method described as solving an elliptic equation with variable coefficients, Eq. (31), in a periodic cylinder, Eq. (14). The method can also be applied to implicit time differencing of parabolic problems. It is particularly attractive if the coefficients are time independent, for then, the time-consuming part of the calculation needs to be done only once.

Appendix A

In this section, we present the generation of the matrix A from the vector of harmonics a. If two functions u and a have $1-D$ Fourier series representations,

$$u(v) = \sum_{k=0}^{N} u_k \cos kv + v_k \sin kv \tag{A-1a}$$

and

$$a(v) = \sum_{k=0}^{N} a_k \cos kv + b_k \sin kv, \tag{A-1b}$$

then the product au has a series representation whose leading terms are

$$(au)(v) = \sum_{k=0}^{N} c_k \cos kv + d_k \sin kv, \tag{A-2}$$

where

$$c_0 = a_0 u_0 + \left(\frac{1}{2}\right) \sum_{j=1}^{N} (a_j u_j + b_j v_j). \tag{A-3}$$

For $n \geqslant 1$, let $n_1 = \min\{n-1, N-n\}$. Then

$$2c_n = \sum_{j=0}^{n_1} (a_{n-j} + a_{n+j})\, u_j + (b_{n+j} - b_{n-j})\, v_j + z \tag{A-4a}$$

and

$$2d_n = \sum_{j=0}^{n_1} (b_{n-j} + b_{n+j})\, u_j + (a_{n-j} - a_{n+j})\, v_j + w. \tag{A-4b}$$

The trailing terms z, w depend on one of the following: If $N - n < n$,

$$z = \sum_{j=N-n+1}^{n-1} (a_{n-j} u_j - b_{n-j} v_j) + 2a_0 u_n + \sum_{j=n+1}^{N} (a_{j-n} u_j + b_{j-n} v_j), \tag{A-5a}$$

and

$$w = \sum_{j=N-n+1}^{n-1} (b_{n-j} u_j + a_{n-j} v_j) + 2a_0 v_n + \sum_{j=n+1}^{N} (-b_{j-n} u_j + a_{j-n} v_j). \tag{A-5b}$$

If $N - n = n$,

$$z = (2a_0 + a_N) u_n + b_N v_n + \sum_{j=n+1}^{N} (a_{j-n} u_j + b_{j-n} v_j), \tag{A-6a}$$

and

$$w = b_N u_n + (2a_0 - a_N)\, v_n + \sum_{j=n+1}^{N} (-b_{j-n} u_j + a_{j-n} v_j). \tag{A-6b}$$

If $N - n > n$,

$$\begin{aligned} z = (2a_0 + a_{2n}) u_n + b_{2n} v_n + \sum_{j=n+1}^{N-n} & [(a_{j+n} + a_{j-n}) u_j \\ & + (b_{j+n} + b_{j-n}) v_j] + \sum_{j=N-n+1}^{N} (a_{j-n} u_j + b_{j-n} v_j), \end{aligned} \tag{A-7a}$$

and

$$w = b_{2n}u_n + (2a_0 - a_{2n})v_n + \sum_{j=n+1}^{N-n} [(b_{n+j} - b_{j-n})u_j + (a_{j-n} - a_{j+n})v_j] + \sum_{j=N-n+1}^{N} (-b_{j-n}u_j + a_{j-n}v_j). \tag{A-7b}$$

In two- (and higher) dimensions, the above algorithm is reapplied. Suppose a and u have $2-D$ expansions in two variables μ, ν as in Eq. (27). In Eq. (A-1) above, assume that u_k, v_k, a_k, b_k are functions of μ, each with its own series expansion (in μ). The expressions in Eqs. (A-3) to (A-7) now correspond to series multiplications. For example, in Eq. (A-4a) the vector of harmonics multiplying the vector $u_1(\mu)$ is $(a_{n-1}(\mu) + a_{n+1}(\mu))$. One repeats the above procedure to compute the $c_{n,1}$ subblock.

Generalization to $n > 2$ dimensions is straightforward.

Appendix B

We now justify the apparently arbitrary modification of the first row of the matrix as described in Section 4C.

Let $\mathbf{M}X = y$ denote the linear system consisting of Eqs. (39), (31) and (33), and let m denote the order of $\mathbf{M}$. Since the Neumann problem is unique up to a constant, $\mathbf{M}$ has rank $m-1$. The augmented system obtained by adding the discretization of Eq. (20), is of rank m. Thus, to justify our elimination of the first row of Eq. (39), we must show that the first row of $\mathbf{M}$ is linearly dependent on the other rows. It is proven below that the addition of the number "one" to the (1, 1) element of $\mathbf{M}$ results in a nonsingular matrix. Hence rows 2 through m are linearly independent, so that the first row does indeed depend linearly on the others. The proof that adding one to the (1, 1) element of $\mathbf{M}$ results in a nonsingular matrix follows.

Consider the following elliptic problem for u in a toroidal domain D:

$$\nabla^2 u = f \qquad \text{in } D, \tag{B-1a}$$

$$\partial u/\partial n = g \qquad \text{on } \partial D. \tag{B-1b}$$

Using the identity

$$\int_D \nabla^2 u \, dv - \int_{\partial D} \frac{\partial u}{\partial n} da = 0, \tag{B-2}$$

it follows that the functions f and g must satisfy an integral equation in order for u to exist. Analogously, the Neumann problem for χ has a solution because of the discussion following Eq. (11).

Using the Fourier expansion method, Eqs. (B-1) are transformed into a linear system

$$\bar{M}\bar{\chi} = \bar{y}. \tag{B-3}$$

In Eq. (B-3), we include *all* the unknown values of χ. Using the representation of Section 4B,

$$\bar{\chi}^T = (x_0, \chi_1, ..., \chi_{L+1}), \tag{B-4}$$

where $\dim(x_0) = N + 1$; and for $i = 1, ..., L + 1$, $\dim(\chi_i) = (M + 1)(N + 1)$.

Define $m = \dim(\bar{\chi})$. The sub-vector x_0 contains the unknown harmonics at $\sigma = 0$. The sub-vectors $\bar{\chi}_i$ $(i = 1, ..., L)$ contain the harmonics at $\sigma = \sigma_i$ where $\sigma_L = 1$; while χ_{L+1} contains the harmonics at the "image tube" $\sigma = 1 + \Delta\sigma_L$. Analogously,

$$\bar{y}^T = (\mu_0, y_1, ..., y_{L+1}). \tag{B-5}$$

The matrix $\bar{M}$ is nearly block tridiagonal. Its first block now consists of Eq. (39). The next L block rows consist of the appropriate matrices in Eq. (31). For $j = 1$, Q_1 is transformed as per the discussion following Eq. (40). The last block row is Eq. (33), and breaks the block tridiagonal structure.

The matrix $\bar{M}$ is the discretization of the differential operators in Eqs. (B.1). The solution to this is unique only up to an additive constant. Hence, $\bar{M}$ is singular and for arbitrary $\bar{y}$, Eq. (B-3) has either

(1) an infinite number of solutions, or

(2) no solutions.

Using the vector format of Eq. (B-4), consider the m-dimensional vector $\bar{v}$ consisting of subvectors v_i which have all zero elements except for a unit first element. This vector is the analogue of a constant function (=1) in the Fourier harmonic representation. The constant function satisfies Laplace's equation with homogeneous boundary conditions. Since $\bar{M}$ is a consistent discretization of the Neumann problem,

$$\bar{M}\bar{v} = 0 \tag{B-6}$$

Case (1) above is thus explained; if for some $\bar{y}$, $\bar{\chi}$ solves Eq. (B-3), then $\bar{\chi} + \alpha\bar{v}$ is another solution where α is an arbitrary constant. In algebraic terms, $\bar{v}$ spans the null space of the operator $\bar{M}$. The second case arises if the $\bar{y}$ vector, which is the Fourier representation of the functions f and g in Eq. (B-1), does not satisfy the discretization of Eq. (B-2).

Define a square matrix **N** with order (**N**) = order (**M**). Using the matrix format for **M**, let **N** consist of all zeros except for "1" in the (1, 1) element of the last diagonal

block. For an arbitrary vector $\bar{\chi}$, $\mathbf{N}\bar{\chi}$ is a vector with at most one non-zero element. Recalling Eq. (27), at $\sigma = 1 + \Delta\sigma_L$,

$$\chi(\sigma = 1 + \Delta\sigma_L) = \chi_{0,0}(\sigma_{L+1}) + \sum_{k,l}{}' \chi_{k,l}(\sigma_{L+1}) \exp(i(k\phi + l\zeta)) \tag{B-7}$$

where the prime signifies that the average value ($k = 0 = l$) is excluded from the sum. The requirement that

can be expressed in matrix-vector form

$$\mathbf{N}\bar{\chi} = \gamma_{L+1}\bar{w} \tag{B-9}$$

where $\bar{w}$ is an m-dimensional vector with only one non-zero element.

The solution to the Neumann problem, Eq. (B-3) (for an appropriately chosen $\bar{y}$) can be made unique by incorporating Eq. (B-9). Define a new matrix (operator)

$$\mathbf{M}' = \mathbf{M} + \mathbf{N}.$$

Any vector $\bar{\chi}$ satisfying Eqs. (B-3) and (B-9) satisfies

$$\mathbf{M}'\bar{\chi} = \bar{y} + x_{L+1}\bar{w}. \tag{B-10}$$

We now show that the operator $\mathbf{M}'$ is invertable by proving that if $\bar{u} \neq 0$ then $\mathbf{M}'\bar{u} \neq 0$. This proves that the modified problem, Eq. (B-10), can be solved. Consider any such $\bar{u}$, which we subdivide as in Eq. (B-4). Let u_l be the first element of the sub-vector $\bar{u}_{L+1}$. Define the vector

$$\bar{s} = \bar{u} - u_l\bar{v}, \tag{B-11}$$

a vector which has at least one zero element. Then

$$\begin{aligned}\mathbf{M}'\bar{u} &= (\mathbf{M} + \mathbf{N})(\bar{s} + u_l\bar{v}) \\ &= \mathbf{M}\bar{s} + u_l\mathbf{M}\bar{v} + \mathbf{N}\bar{s} + u_l\mathbf{N}\bar{v}.\end{aligned} \tag{B-12}$$

The second term vanishes because of Eq. (B-6); the third because $\bar{s}$ is chosen to have zero in the crucial element. The last element vanishes only if $u_l = 0$; the first term vanishes only if $\bar{s}$ is a multiple of $\bar{v}$ — mutually exclusive possibilities. Since by assumption $\bar{u} = 0$, our proof that Eq. (B-12) is non-zero is complete if we can show

$$\mathbf{M}\bar{s} \neq -u_l\mathbf{N}\bar{v}. \tag{B-13}$$

We prove this by contradiction. Since $u_l \neq 0$, the r.h.s. of Eq. (B-13) is zero except for one element. An equality in Eq. (B-13) corresponds to the discretization of Eqs.

(B-1) with $f \equiv 0$ and $g \equiv u_l = \text{const}$ since $\mathbf{M}\bar{s}$ corresponds to a consistent discretization of Eqs. (B-1). This is impossible since the compatibility condition would then be violated, i.e.,

$$\int_{\partial D} g \, da = u_l \int_{\partial D} da = u_l \, \text{Area}(\partial D) \neq 0.$$

This completes the proof that if $u \neq 0$, $\mathbf{M}'u \neq 0$. Hence, $\mathbf{M}'$ can be inverted.

The above proof can be repeated when the average value of χ is prescribed at another $\sigma = \text{value}$. Beginning with Eq. (B-7), using similar arguments, one needs to reprove Eq. (B-13) where the location of the lone non-zero element of $\mathbf{N}$ is different. In this case the corresponding boundary function g vanishes while the function f (see Eq. (B-1a)) is zero except at some internal value of σ. It is easy to show that for this f and g Eq. (B-2) cannot hold. Thus, no vector $\bar{s}$ can render equality in Eq. (B-13). This proves that the modified $\mathbf{M}'$ always has an inverse when one is added to the (1, 1) elements of any its diagonal blocks. Consequently, as discussed in the beginning of this appendix, it is allowable to perform the row replacement as in Section 4C.

ACKNOWLEDGMENTS

The authors wish to thank Dr. Harold Furth of the Princeton Plasma Physics Laboratory for suggesting the problem to them and for his continued support and encouragement. They also thank Dr. O. Betancourt of New York University and Dr. W. Dommaschk of Max–Planck-Institut für Plasmaphysik for graciously providing valuable reprints of their work. The authors profited from fruitful discussions with Drs. S. Yoshikawa and T. K. Chu of Princeton. Their interest in this project gave much stimulus. The field line solver which calculated the magnetic surfaces was an important part of evaluating the resulting solution. Many thanks go out to Mr. N. O'Neill for making the many necessary modifications to the existing code TUBE. The original paper was improved after incorporating the suggestions of the referees.

REFERENCES

1. *Physics Today* (August 1980), 17.
2. A. H. BOOZER *et al.*, *in* "Plasma Physics and Controlled Nuclear Fusion Research 1982, Ninth Conference Proceedings, Baltimore, USA, September 1–8, 1982." Nuclear Fusion, Supplement 1983, 111–129.
3. S. YOSHIKAWA, Princeton Plasma Physics Laboratory, private communication, 1981.
4. J. M. GREENE AND J. L. JOHNSON, *in* "Advances in Theoretical Physics" (K. A. Brueckner, Ed.), Vol. 1, Academic Press, New York, 1965.
5. A. B. EHRHARDT, *Bull. Amer. Phys. Soc.* **28**, No. 8; Proceedings, 25th Annual Meeting of the Division of Plasma Physics in Los Angeles, CA; Nov. 7–11, 1983, paper 1F4.
6. J. D. JACKSON, "Classical Electrodynamics," Wiley, 2nd ed., New York, 1975.
7. L. P. MAI, G. GIBSON, AND T. K. CHU, *in* "Proceedings' Fourth U. S. Stellarator Workshop, Oak Ridge National Laboratory, Oak Ridge, TN, April 14–15, 1983," CONF-830428.

8. W. DOMMASCHK, *Z. Naturforsch A* **36** (1981), 251–260.
9. W. DOMMASCHK AND J. NUHRENBERG, Max Planck Institute fur Plasmaphysik, private communication, 1983.
10. O. L. BETANCOURT, "Three Dimensional Computation of Magnetohydrodynamic Equilibrium of Toroidal Plasma without Axial Symmetry," Courant Institute of Mathematical Sciences, New York University, AEC Research and Development Report, C00-3077-49, MF-67, June 1974.
11. P. R. GARABEDIAN, "Partial Differential Equations," Wiley, New York, 1964.
12. A. C. HINDMARSH, "Solution of Block-Tridiagonal Systems of Linear Algebraic Equations," Lawrence Livermore National Laboratory, UCID-30150, February 1977.
13. A. GREENBAUM, Lawrence Livermore National Laboratory, private communication, 1983.
14. A. I. SHESTAKOV, A. A. MIRIN, AND N. O'NEILL, *in* "Proceedings, Fourth U.S. Stellarator Workshop, Oak Ridge National Laboratory, Oak Ridge Tenn., April 14–15, 1983."
15. N. O'NEILL AND A. MIRIN, TUBE-*a* Field Line Integrator Code, LIBRIS abstract P81, Magnetic Fusion Energy Computer Center, Lawrence Livermore National Laboratory, Livermore, CA.
16. H. RENNER, D. J. LEES, AND T. K. CHU, *IEEE Trans. Plasma Sci.* **PS-9**, No. 4, (1981).
17. J. NÜHRENBERG AND U. SCHWENN, Max–Planck-Institute-für-Plasmaphysik, private communication, 1983.